Journal of Alloys and Compounds 504 (2010) 542–547

Contents lists available at ScienceDirect

Journal of Alloys and Compounds

journal homepage: www.elsevier.com/locate/jallcom

Effect of submicron size SiC particulates on microstructure and mechanical properties of AZ91 magnesium matrix composites

K.K. Deng*, K. Wu, Y.W. Wu, K.B. Nie, M.Y. Zheng

School of Material Science and Engineering, Harbin Institute of Technology, No.92, West Da-Zhi Street, Harbin 150001, PR China

ARTICLE INFO

Article history:
Received 9 March 2010
Received in revised form 25 May 2010
Accepted 29 May 2010
Available online 11 June 2010

Keywords:
Submicron-SiC particulate
Magnesium matrix composite
Microstructure
Mechanical property

ABSTRACT

In the present study, AZ91 magnesium matrix composites reinforced with six volume fractions (0.5, 1, 1.5, 2, 3 and 5 vol.%) of submicron-SiC particulates (0.2 μm) were fabricated by stir casting. The as-cast ingots were forged at 420 °C with 50% reduction, and then extruded at 370 °C with the ratio of 16 at a constant ram speed of 15 mm/s. The microstructure of the composites was investigated by optical microscopy, scanning electron microscope and X-ray diffractometer. Microstructure characterization of the composites showed relative uniform reinforcement distribution, significant grain refinement and presence of minimal porosity. The X-ray diffractometer analysis showed that a strong basal plane texture was formed in both AZ91 alloy and SiCp/AZ91 composites during extrusion and the addition of submicron-SiC particulates could weaken the basal plane texture. The presence of submicron-SiC particulates assisted in improving the thermal stability, micro-hardness, elastic modulus and 0.2% yield strength. Both of the 0.2% yield strength and ultimate tensile strength increased with the increasing of submicron-SiC particulate content, however, decreased as the SiC particulate content overrun 2 vol.%.

1. Introduction

Magnesium is paid more attention as light metals and alloys, due to its intrinsic characteristics of low density, good machineability and availability in the global market [1,2]. However, the application of magnesium is limited because of its low strength, poor room temperature ductility and toughness. Since magnesium matrix composites exhibit many advantages over monolithic magnesium or magnesium alloys, such as high elastic modulus, high strength, superior creep and wear resistances at elevated temperatures [3], numerous studies have been made on magnesium matrix composites. Hassan and Gupta [4,5] investigated the microstructure and tensile properties of elemental Mg reinforced with Al_2O_3 particulates. Wang et al. [6] improved the yield strength of MgLiAl matrix composite through the addition of YAl_2 particulates. Nguyen and Gupta [7] fabricated AZ31B–3.3Al_2O_3–Cu composite using disintegrated melt deposition technique, and it was found that the addition of nano-Al_2O_3 and Cu led to a simultaneous improvement in 0.2% yield compressive strength, ultimate compressive strength and work of fracture of the AZ31B magnesium.

Smaller ceramic particulates with a little amount volume fraction have significant influence on microstructure and mechanical properties of particulate reinforced magnesium matrix composites. Chen et al.'s [8] study illustrated that a little amount of 1–2 μm SiC particulates had great effect on grain refinement of AZ91D magnesium alloy. And Saberi's [9] research illustrated that the role of nano-size SiC on grain refinement was much more significant than that of micron size. On Radi and Mahmudi's [10] research of nano-Al_2O_3/AZ31 magnesium matrix composite fabricated by stir casting, nano-Al_2O_3 particulates could pin grain boundary and interact with dislocations to increase the friction stress. Habibnejad-Korayem et al. [11] fabricated nano-Al_2O_3/Mg composites by stir casting method, and it was found that the addition of nano-particulates resulted in significant improvement on tensile properties of both Mg and AZ31 composites due to the coefficient of thermal expansion mismatch between the matrix and the particulates, a lesser extent to the Orowan and Hall–Petch strengthening mechanisms. Recently, some investigation has been made on nano-size particulate reinforced magnesium matrix composites, however, because of higher cost of nano-size particulates, it is potential and more economical to study submicron size particulates reinforced magnesium matrix composites. So far, no attempt is made to study in detail the effects of submicron-SiC particulates on microstructure and mechanical properties of magnesium matrix composites. Smaller particulate reinforced composites had been produced by a variety of methods: stir casting [6,10–13], disintegrated melt deposition [7], powder metallurgy [2,14], etc. However, stir casting method is preferred to other techniques for its capability in producing complex shapes at a high production rate and low costs.

* Corresponding author. Tel.: +86 451 86402291; fax: +86 451 86413922.
E-mail address: jamsdk@163.com (K.K. Deng).

0925-8388/$ – see front matter © 2010 Elsevier B.V. All rights reserved.
doi:10.1016/j.jallcom.2010.05.159

Table 1
The chemical compositions (wt.%) of the AZ91 magnesium alloy.

Al	Zn	Mn	Si	Cu	Ni	Fe	Be	Mg
9.3	0.7	0.23	0.02	0.001	0.001	0.002	0.0015	Balance

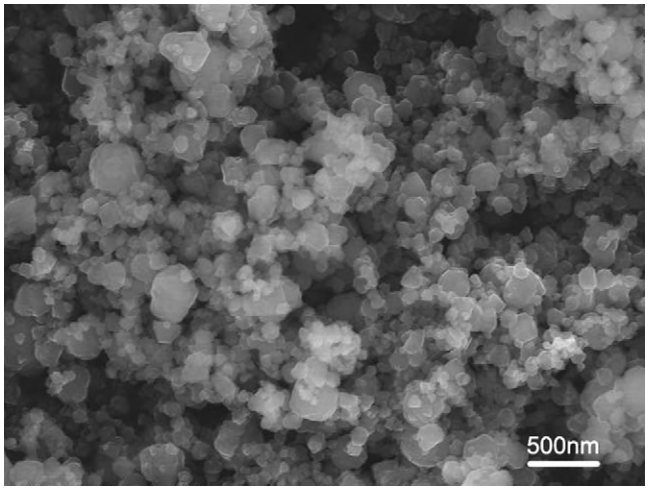

Fig. 1. SEM image of the submicron-SiC particulates.

Accordingly, the primary aim of the present study is to fabricate magnesium matrix composite reinforced with different volume fraction of 0.2 μm sized SiC particulates by stir casting, and then studies the effect of the presence of submicron-SiC particulates and its increasing amount on the microstructure and mechanical properties of magnesium matrix composite.

2. Experimental procedures

2.1. Materials

AZ91 magnesium alloy (supplied by Northeast Light Alloy Company Limited, China) was selected as matrix alloy, and the chemical compositions of AZ91alloy are given in Table 1. SiC particulates (supplied by White Dove Company Limited, China) with the average size of 0.2 μm were used as reinforcement, and the SEM image of the submicron-SiC particulates is shown in Fig. 1.

2.2. Fabrication of the composite

The SiC particulates reinforced AZ91 magnesium matrix composites (SiCp/AZ91) containing six volume fractions (0.5, 1, 1.5, 2, 3 and 5 vol.%) were fabricated by stir casting. The whole fabrication process was conducted in a protective atmosphere of CO_2 and SF_6 to avoid burning. The AZ91 alloy was molten at 720 °C, and then cooled to 590 °C which made the matrix alloy in the semi-solid condition. As the SiC particulates were added into the molten AZ91 alloy, the melt was stirred for 30 min, and then was rapidly reheated to 720 °C for casting. The melt was poured into a preheated steel mould (450 °C) and solidified under a 100 MPa pressure to reduce the porosity of composite ingots.

2.3. Secondary processing

The monolithic AZ91 alloy and SiCp/AZ91composites ingots were machined to 57 mm in diameter after solutionized at 415 °C for 24 h, and forged to 80 mm in diameter with 50% reduction on height at 420 °C. Subsequently, the forged alloy and composites were extruded at 370 °C with the ratio of 16 at a constant ram speed of 15 mm/s. Rods of 20 mm in diameter were obtained following extrusion.

2.4. Density measurement

Density (ρ) measurements were performed in accordance with Archimedes' principle on three randomly selected polished samples of AZ91 alloy and SiCp/AZ91composites taken from the extruded rods. Distilled water was used as the immersion fluid. The samples were weighed using a TG328A analytical balance, with an accuracy of ±0.0001 g. Theoretical densities of materials were calculated to measure the volume percentage of porosity of materials. Rule of mixture was used in both calculations.

2.5. Microstructure characterization

Microstructure observation was carried out by optical microscopy (OM) and scanning electron microscope (SEM). Microstructure observation plane was cut parallel to extrusion direction. The specimens for OM were ground, polished and then etched in acetic picral [5 ml acetic acid + 6 g picric acid + 10 ml H_2O + 100 ml ethanol (95%)] to investigate morphological characteristics of grains. The average grain size was measured using the linear intercept method. The specimens for SEM were ground and polished to investigate reinforcement distribution and interfacial integrity between the matrix and reinforcement.

2.6. X-ray diffraction studies

The intensity of basal plane texture of AZ91 alloy and SiCp/AZ91composites was tested by X-ray diffractometer (XRD). The specimens of XRD were conducted on the plane parallel to extrusion direction.

2.7. Coefficient of thermal expansion

The coefficients of thermal expansion (CTE) of the extruded AZ91 alloy and SiCp/AZ91composites were determined by measuring the displacement of the samples as a function of temperature in the temperature range 50–300 °C using an automated NETZSCH DIL 402C thermo-mechanical analyzer.

2.8. Micro-hardness

The AZ91 alloy and submicron-SiCp/AZ91composites were characterized using Vickers hardness measurements with a load of 0.2 kg. Each micro-hardness value is the average of at least five measurements.

2.9. Tensile testing

The tensile specimens were cut parallel to extrusion direction, and the tensile test was carried out on an Instron Series 5569 test machine at room temperature with the tensile rate of 0.5 mm/min.

3. Results and discussion

3.1. Microstructure observation

The density and porosity of submicron-SiCp/AZ91composites is shown in Table 2. Although a little amount of porosity exists in the composites, the near dense composites are obtained due to the reasonable experimental parameters during forging and extrusion process. Table 2 illustrates that the porosity of the composites

Table 2
Results of density, porosity and CTE of AZ91 alloy and submicron-SiCp/AZ91composites.

Materials	SiC (vol.%)	Density (g/cm^3)		Porosity (%)	CTE (10^{-6}/°C)
		Theoretical	Experimental		
AZ91	0	1.81	1.8099 ± 0.0001	0.00562	28.9192
0.5SiC/AZ91	0.5	1.8169	1.81645 ± 0.00132	0.02486	28.0732
1SiC/AZ91	1	1.8238	1.82278 ± 0.00214	0.056	27.368
1.5SiC/AZ91	1.5	1.8307	1.82924 ± 0.00161	0.07948	27.2279
2SiC/AZ91	2	1.8376	1.83564 ± 0.00096	0.10673	26.6346
3SiC/AZ91	3	1.8514	1.84885 ± 0.00186	0.13749	26.162
5SiC/AZ91	5	1.879	1.87388 ± 0.00217	0.2726	25.765

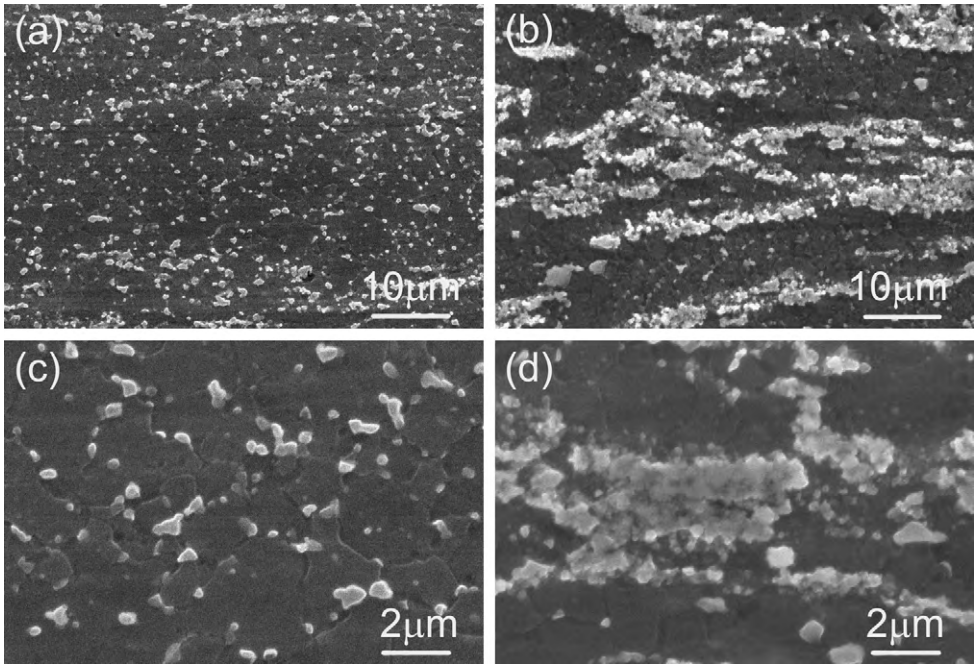

Fig. 2. SEM of submicron-SiC particulate distribution in the extruded submicron-SiCp/AZ91 composites: (a) and (c) 0.5 vol.% SiCp/AZ91; (b) and (d) 5 vol.% SiCp/AZ91; (c) high magnification of (a); (d) high magnification of (b).

slightly increases with increasing volume fraction. And the reason could be explained as follows: gas could enter into the molten liquid at the stirring stage during fabrication process of composites. The pore could nucleate at SiC particulate sites and the contact surface area increases with the SiC particulate volume fraction increase, which leads to the increase of porosity level [13].

The SEM micrographs of submicron-SiCp/AZ91 composites are presented in Fig. 2. Fig. 2(a) is the typical image of this composite in low magnification. It could be found that the submicron-SiC particulates distribute relative homogeneous in composite matrix. And the reasons can be attributed to: (1) good dispersion of submicron-SiC particulates in the AZ91 magnesium alloy matrix during stir

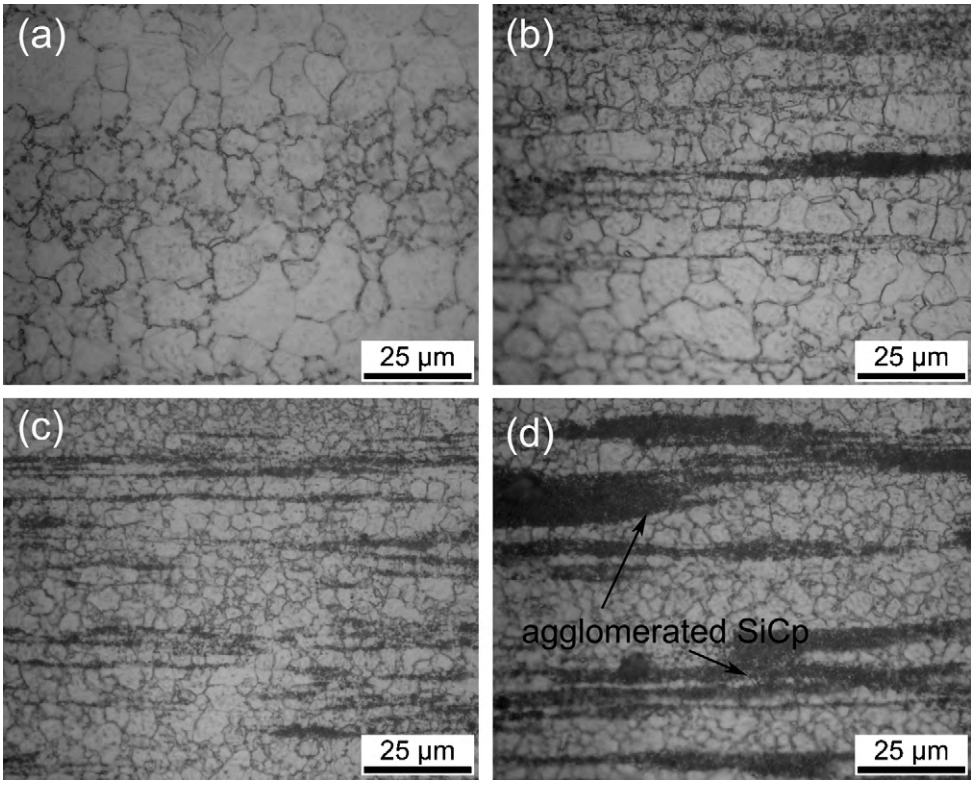

Fig. 3. Optical micrographs of extruded (a) AZ91 alloy and submicron-SiCp/AZ91 magnesium matrix composites reinforced with (b) 0.5 vol.%, (c) 2 vol.% and (d) 5 vol.% SiC particulates.

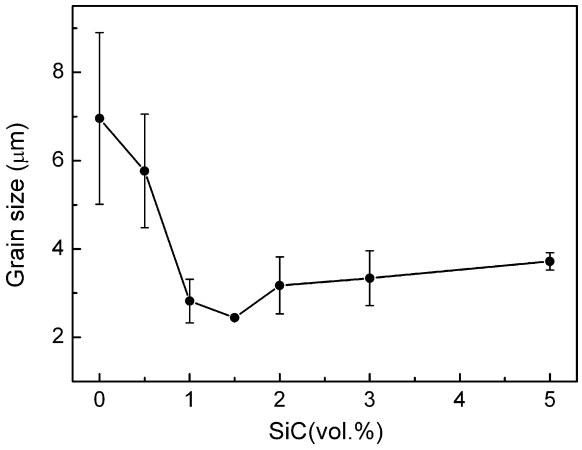

Fig. 4. The grain size of submicron-SiCp/AZ91 magnesium matrix composites with different volume fractions.

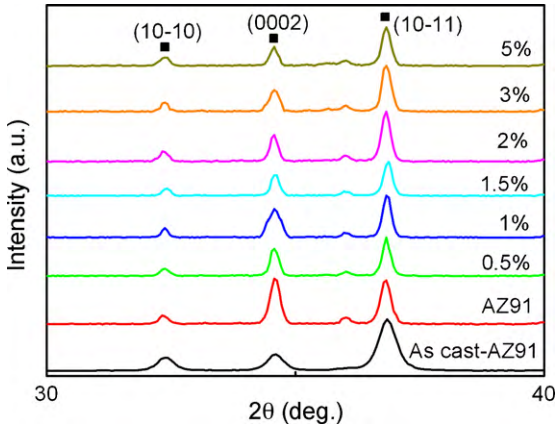

Fig. 5. X-ray diffraction patterns of AZ91 and submicron-SiCp/AZ91composites with different volume fractions.

casting; and (2) good wetting between submicron-SiC particulates and AZ91 alloy. The higher magnification of submicron-SiC particulates is shown in Fig. 2(c). It illustrates that the good interfacial bonding between matrix and SiC particulates is obtained in the composite [4,5,13,15]. The agglomerating regions are found in the composite with the higher volume fraction of SiC particulates, and the images are shown in Fig. 2(b) and (d).

The results of microstructure characterization reveal the presence of nearly equiaxed grains in both monolithic alloy and composites in all samples, as shown in Fig. 3. The addition of submicron-SiC particulates has significant effect on reducing grain size. And the effect of submicron-SiC particulate content on the grain size of composites is shown in Fig. 4. The grain size decreases with the increase of SiC particulates content at certain volume fraction, and then increases with the continuous increase of volume fraction. The minimum value of grain size obtained in certain volume fraction of submicron-SiC particulates could be attributed to two reasons: (1) SiC particulates may induce recrystallisation of the magnesium matrix through stimulation of nucleation at the SiC/Mg interfaces during hot deformation [16,17], and the added SiC particulates could restrict the grain growth as the increasing of volume fraction. (2) The effect of restriction is weakened as the volume fraction of submicron-SiC particulates increased to 5% due to the increasing of agglomerating regions, which lead to the grain growth as the volume fraction continues increasing.

3.2. Texture evolution

Fig. 5 shows the X-ray diffraction spectra of monolithic AZ91 alloy and submicron-SiCp/AZ91 magnesium matrix composites. Compared to the X-ray diffraction spectra of as cast and as extruded AZ91 alloy, the peak of basal plane is much higher after extrusion, which means that the strong basal plane texture formed in AZ91 alloy during extrusion. It has been reported that a strong basal plane texture could be formed in magnesium alloys during extrusion due to limitation in slip systems [18–20]. Besides, on Garcés et al.'s work of Mg–Y_2O_3 composites [21] and Mg–SiCp composites [22], all the materials show the typical extrusion texture of magnesium alloys with basal plane parallel to the extrusion direction.

In order to study the effect of submicron-SiC particulates contents on the change of the basal plane texture, $I_{(0002)}$ and $I_{(10-10)}$ are chosen to denote the intensity of basal plane peak and pyramidal plane peak, respectively. So the relative intensity of basal plane peak could be got by $I_{(0002)}/I_{(10-10)}$. Fig. 6 shows the $I_{(0002)}/I_{(10-10)}$ values of SiC/AZ91composites with different volume fractions. The $I_{(0002)}/I_{(10-10)}$ value of basal plane in the composite is lower than that of monolithic AZ91 alloy, which means that the intensity of basal plane texture weakened with the addition of SiC particulates. And the value of $I_{(0002)}/I_{(10-10)}$ decreases as the increasing of SiC particulate contents. This phenomenon has also been reported by Garcés et al.'s work on Mg–Y_2O_3 composites [21] and Mg–SiCp composites [22]. The weakening of basal plane texture with the increasing of SiC particulate contents can be explained by the following reasons: on one hand, the smaller grain size of the composites compared with monolithic AZ91 alloy may indicate recrystallisation occurred in the magnesium matrix, as mentioned above, and recrystallisation weakens the basal plane texture of AZ91 matrix; on the other hand, the elongated agglomerating regions of submicron-SiC particulates are found orientated in the extrusion direction, which indicates that the agglomerating regions of SiC particulates caused by increasing volume fraction inhibit the plastic flow of AZ91 matrix. The AZ91 alloy has to flow around the particulates and change the initial orientation, which weakens the basal plane texture.

3.3. Thermal behavior

The results of CTE shown in Table 2 reveal that the average CTE values of the SiCp/AZ91composites decrease as the increasing of submicron-SiC particulates. The results suggest an appropriate integration of AZ91 alloy with low CTE submicron-SiC particulates. The results are consistent with the similar findings made by investigations on other magnesium matrix composites con-

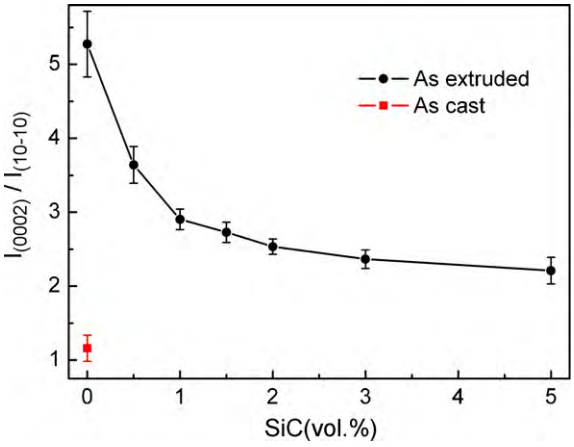

Fig. 6. The $I_{(0002)}/I_{(10-10)}$ values of AZ91 and submicron-SiCp/AZ91 composites with different volume fractions.

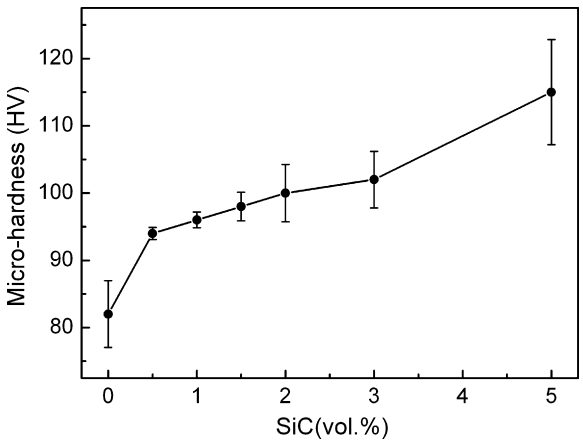

Fig. 7. Variation of micro-hardness as function of submicron-SiC particulate contents.

taining different types of reinforcements and in different length scales [4,5]. The lower CTE values of SiCp/AZ91 composites could be attributed to the large difference between submicron-SiC particulates and AZ91 matrix [23]. The difference between the resistance of the SiC particulates and AZ91 matrix against expansion makes submicron-SiC particulates constrain the expansion of the composites during heating [11,23]. Consequently, the average CTE of SiCp/AZ91 composite is reduced as the volume fraction of SiC particulates increases.

3.4. Mechanical properties

A prominent increase in micro-hardness is observed in the SiCp/AZ91 composites as compared to un-reinforced AZ91 alloy, as shown in Fig. 7. The micro-hardness of submicron-SiCp/AZ91 composites increases with the increasing of volume fraction of particulates. The increase in the micro-hardness of submicron-particulates reinforced composites can be attributed to the following reasons: (1) the submicron-SiC particulates are harder than magnesium alloy and render their inherent property of hardness to the soft matrix; (2) the submicron-SiC particulates act as obstacles to the motion of dislocation; and (3) the micro-hardness increment can also be attributed to the grain refinement, as shown in Fig. 3.

The elastic modulus of AZ91 matrix is improved due to the addition of submicron-SiC particulates, as shown in Fig. 8. The increased elastic modulus of AZ91 matrix is mainly attributed

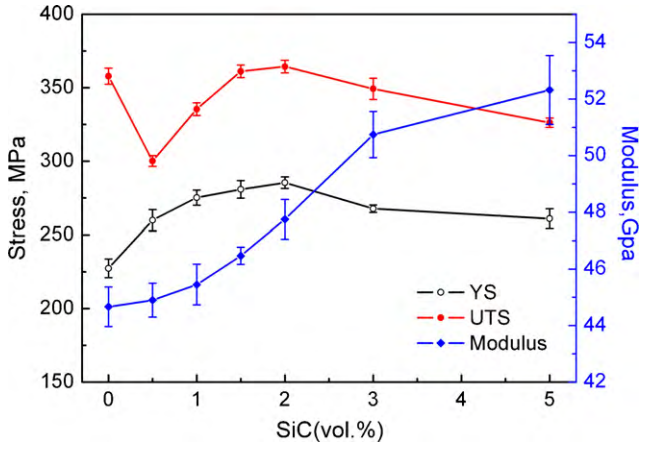

Fig. 8. The tensile properties of extruded AZ91 alloy and submicron-SiCp/AZ91 magnesium matrix composites.

to the high modulus of added SiC particulates and good interfacial integrity between particulates and matrix. It may be noted that good matrix–reinforcement interfacial integrity leads to a significant increase in internal stress between reinforcement and matrix resulting in the enhancement of elastic modulus [24]. And the elastic modulus of submicron-SiCp/AZ91 magnesium matrix composites increases as the increasing of SiC particulate contents, which has the same changing trend of micro-hardness.

Tensile properties of AZ91 and submicron-SiCp/AZ91 magnesium matrix composites are shown in Fig. 8. The results of ambient temperature tensile tests reveal obvious improvement in 0.2% yield strength (YS) of AZ91 matrix due to the presence of submicron-SiC particulates. The increase in 0.2% YS can primarily be attributed to grain refinement, the strong multidirectional thermal stress at the SiC/Mg interface, small particle size and low degree of porosity which lead to effective transfer of applied tensile load to the SiC particulates.

Fig. 8 also shows that the quiet significant improvement in 0.2% YS of AZ91 matrix is obtained as 2 vol.% SiC particulates are added. It could be attributed to the grain refinement caused by the increasing of volume fraction of SiC particulates. In general, the yield strength of a polycrystalline material increases with the decrease of grain size according to Hall–Petch relation. Besides, the increased submicron-particulates can also induce heavily built multidirectional thermal stress at the particulate/matrix interface at grain boundaries due to the large difference of coefficient of thermal expansion between matrix and reinforcement, and induce high dislocation density with the increase of particulates contents [13]. And all of these reasons lead to the significant increase in the yield strength of the composites over monolithic AZ91alloy. However, further increase in SiC particulates content from 2 to 5 vol.% lead to reduction in the 0.2% YS values of AZ91 matrix. This significance could be attributed to the increasing agglomerating regions as the increasing SiC particulate contents, as shown in Fig. 2(b) and (d), which weaken the strengthened effect of SiC particulates. Besides, the grain size increases as the increasing of SiC particulate contents from 2% to 5%, as shown in Fig. 4, which is also the reason for the decreasing 0.2% YS of AZ91 matrix.

Compared to un-reinforced AZ91 alloy, the 0.2% YS of composite increases but the ultimate tensile strength (UTS) decreases due to the addition of reinforcements. Actually, this phenomenon has been reported by Seshan et al.'s [25] work on two magnesium alloys reinforced with SiC particulates. The lower UTS value of composite with SiC fraction of 0.5% than that of the un-reinforced AZ91 alloy can be attributed to the following reasons: on one hand, the degradation of UTS could arise from the influences of residual stress produced during deformation process [25]; on the other hand, it could be attributed to the failure of agglomerated submicron-SiC particulates. Fig. 9 shows the fracture surface of AZ91 alloy and SiCp/AZ91 magnesium matrix composites. A little amount of agglomerated submicron-SiC particulates still exist in 0.5 vol.% SiC/AZ91 composite. The microcracks occur in the agglomerated regions during tensile test, as shown in Fig. 9(b). This might lead to the decrease of UTS compared to un-reinforced AZ91 alloy. The effect of particulates inhibit the crack growth strengthen as the increasing of volume fraction of SiC particulate, which leads to the increase of UTS. However, the agglomerated regions also increase as the volume fraction increase, as shown in Fig. 9(c) and (d). The effect of agglomerated submicron-SiC particulates crack which is higher than the effect of particulate inhibits the crack growth as the volume fraction overrun 2 vol.%. As a result, the UTS decrease as the volume fraction of SiC particulate overrun 2 vol.%.

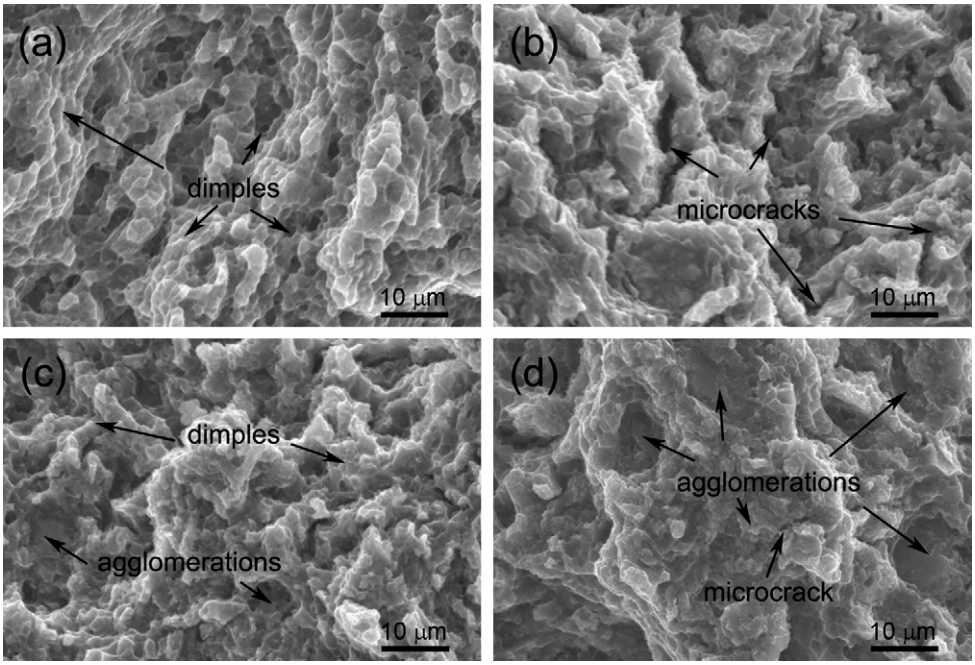

Fig. 9. Fracture surface of extruded (a) AZ91 alloy and submicron-SiCp/AZ91 magnesium matrix composites reinforced with (b) 0.5 vol.%, (c) 2 vol.% and (d) 5 vol.% SiC particulates.

4. Conclusions

(1) The submicron-SiCp/AZ91 composites were fabricated by stir casting and the near dense composites were obtained after the secondary processing.
(2) The submicron-SiC particulates could refine the grain size of AZ91 matrix. The grain size decreased as the SiC particle contents increased to a certain volume fraction, and then increased as the volume fraction further increased to 5%.
(3) A strong basal plane texture formed in both AZ91 alloy and SiCp/AZ91 composites during extrusion and the addition of submicron-SiC particulates could weaken basal plane texture. The value of $I_{(0002)}/I_{(10-10)}$ decreased as the increasing of SiC particulate contents.
(4) The addition of submicron-SiC particulates led to the obvious decrease in CTE of AZ91 matrix, and the CTE of SiCp/AZ91 composites decreased as the increasing of SiC particulate contents.
(5) The 0.2% YS of AZ91 matrix increased significantly; however, the UTS decreased with the addition of a little amount of SiC particulates. Both the 0.2% YS and UTS of SiCp/AZ91 composites increased as the SiC particulate contents increased to 2%, and then decreased as the volume fraction continue increasing to 5% due to the increasing of agglomerated regions and grain growth.
(6) The addition of submicron-SiC particulates led to the increase of micro-hardness and elastic modulus of SiCp/AZ91 composites, and they increased with the increasing of volume fraction of submicron-particulates in the AZ91matrix.

References

[1] B.L. Mordike, T. Ebert, Mater. Sci. Eng. A 302 (2001) 37–45.
[2] Y.V.R.K. Prasad, K.P. Rao a, M. Gupta, Comp. Sci. Technol. 69 (2009) 1070–1076.
[3] P. Poddar, V.C. Srivastava, P.K. De, K.L. Sahoo, Mater. Sci. Eng. A 460–461 (2007) 357–364.
[4] S.F. Hassan, M. Gupta, J. Alloys Compd. 419 (2006) 84–90.
[5] S.F. Hassan, M. Gupta, J. Alloys Compd. 457 (2008) 244–250.
[6] S.J. Wang, G.Q. Wu, Z.H. Ling, Z. Huang, Mater. Sci. Eng. A 518 (2009) 158–161.
[7] Q.B. Nguyen, M. Gupta, J. Alloys Compd. 490 (2010) 382–387.
[8] T.J. Chen, X.D. Jiang, Y. Ma, Y.D. Li, Y. Hao, J. Alloys Compd. 496 (2010) 218–225.
[9] Y. Saberi, S.M. Zebarjad, G.H. Akbari, J. Alloys Compd. 484 (2009) 637–640.
[10] Y. Radi, R. Mahmudi, Mater. Sci. Eng. A 527 (2010) 2764–2771.
[11] M. Habibnejad-Korayem, R. Mahmudi, W.J. Poole, Mater. Sci. Eng. A 519 (2009) 198–203.
[12] A.A. Yar, M. Montazerian, H. Abdizadeh, H.R. Baharvandi, J. Alloys Compd. 484 (2009) 400–404.
[13] A. Mazahery, H. Abdizadeh, H.R. Baharvandi, Mater. Sci. Eng. A 518 (2009) 61–64.
[14] L. Kollo, M. Leparoux, C.R. Bradbury, C. Jäggi, E. Carreño-Morelli, M. Rodríguez-Arbaizar, J. Alloys Compd. 489 (2010) 394–400.
[15] Q.B. Nguyen, M. Gupta, J. Alloys Compd. 459 (2008) 244–250.
[16] K.K. Deng, K. Wu, X.J. Wang, Y.W. Wu, X.S. Hu, M.Y. Zheng, et al., Mater. Sci. Eng. A 527 (2010) 1630–1635.
[17] X.J. Wang, K. Wu, M.Y. Zheng, et al., Mater. Sci. Eng. A 465 (2007) 78–84.
[18] T.T. Sasaki, K. Yamamoto, T. Honma, S. Kamado, K. Hono, Scr. Mater. 59 (2008) 1111–1114.
[19] Y. Uematsu, K. Tokaji, M. Kamakura, K. Uchida, H. Shibata, N. Bekku, Mater. Sci. Eng. A 434 (2006) 131–140.
[20] H.L. Ding, L.F. Liu, S. Kamado, W.J. Ding, Y. Kojima, J. Alloys Compd. 456 (2008) 400–406.
[21] G. Garcés, M. Rodríguez, P. Pérez, P. Adeva, Mater. Sci. Eng. A 419 (2006) 357–364.
[22] G. Garcés, P. Perez, P. Adeva, Scr. Mater. 52 (2005) 615–619.
[23] S.F. Hassan, M. Gupta, J. Mater. Sci. 41 (2006) 2229–2236.
[24] A. Luo, Metall. Trans. A 26 (1995) 2445–2455.
[25] S. Seshan, M. Jayamathy, S.V. Kailas, T.S. Srivatsan, Mater. Sci. Eng. A 363 (2003) 345–351.